Journal of Magnetic Resonance **146,** 126–131 (2000)
doi:10.1006/jmre.2000.2122, available online at http://www.idealibrary.com on IDEAL®

Efficient Measurement of $^3J_{N,C\gamma}$ and $^3J_{C',C\gamma}$ Coupling Constants of Aromatic Residues in ^{13}C, ^{15}N-Labeled Proteins

Frank Löhr and Heinz Rüterjans

Institut für Biophysikalische Chemie, Johann Wolfgang Goethe-Universität Frankfurt, Biozentrum N230, Marie Curie-Strasse 9, 60439 Frankfurt am Main, Germany

E-mail: hruet@bpc.uni-frankfurt.de

Received February 1, 2000; revised May 5, 2000

An NMR pulse sequence is proposed for the simultaneous determination of side chain χ1 torsion-angle related $^3J_{N,C\gamma}$ and $^3J_{C',C\gamma}$ couplings in aromatic amino acid spin systems. The method is of the quantitative *J* correlation type and takes advantage of attenuated ^{15}N and ^1H transverse relaxation by means of the TROSY principle. Unlike previously developed schemes for the measurement of either of the two coupling types, spectra contain internal reference peaks that are usually recorded in separate experiments. Therefore, the desired information is extracted from a single rather than four data sets. The new method is demonstrated with uniformly $^{13}C/^{15}N$ labeled *Desulfovibrio vulgaris* flavodoxin, which contains 14 aromatic out of 147 total amino acid residues.

Key Words: **χ1-angle; quantitative *J* correlation; TROSY; axial peaks; flavodoxin.**

INTRODUCTION

Aromatic residues are very often involved in the construction of the hydrophobic core of proteins. Their side chain conformations in solution can be probed by the measurement of vicinal coupling constants. Unlike scalar interactions involving the pair of C^β-bound protons, analysis of couplings between backbone ^{15}N or $^{13}C'$ nuclei and the aromatic γ-carbon does not depend on stereospecific assignments and chemical shift dispersion of $^1H^\beta$ resonances. Therefore, as was demonstrated recently for unfolded proteins (*1, 2*), $^3J_{N,C\gamma}$ and $^3J_{C',C\gamma}$ provide valuable information about χ1 torsion angle preferences and motional averaging in aromatic residues. The two scalar interactions tend to be relatively small yet readily measurable using recently developed triple-resonance NMR techniques. Their size can be reliably determined with either 2D spin–echo difference (*3*) or 3D quantitative *J* correlation (*4*) experiments, both of which rely on the evaluation of cross peak intensity ratios in different spectra (*5*). Here we propose a three-dimensional pulse sequence which allows a simultaneous determination of both coupling types without the need to record a separate reference spectrum. Application of the TROSY (*6, 7*) methodology ensures high sensitivity, which translates into high precision of the *J* measurement.

RESULTS AND DISCUSSION

The pulse scheme outlined in Fig. 1 is based on the HN(CO)CG (*4, 8*), an "out-and-back" type sequence which transfers magnetization from amide protons of residue *i* to carbonyls of the preceding residue via $^1J_{N,H}$ and $^1J_{N,C'}$. In the central step, dephasing with respect to the long-range C', C^γ coupling of interest occurs during a period ϵ. In t_1, frequency labeling according to the chemical shifts of aromatic γ-carbons, band-selectively excited by the surrounding shaped 90° pulses, takes place. Unlike previous implementations, however, an HMQC- rather than an INEPT-type ^{15}N–$^{13}C'$ transfer is employed, such that additional $^3J_{N,C\gamma}$ dephasing is active for the full period $\delta + \tau_{90°,C'} + \epsilon$. As a result, cross peaks occur at $\omega(^{13}C_i^\gamma)$ and $\omega(^{13}C_{i-1}^\gamma)$ along F_1 with intensities proportional to

$$\sin^2(\pi\,{}^1J_{NC'}\delta) \times \sin^2[\pi\,{}^3J_{NC\gamma(\mathrm{arom},i)}(\delta + \tau_{90°,C'} + \epsilon)] \times \cos^2(\pi\,{}^3J_{C'C\gamma(\mathrm{arom},i-1)}\epsilon) \quad [1]$$

and

$$\sin^2(\pi\,{}^1J_{NC'}\delta) \times \sin^2(\pi\,{}^3J_{C'C\gamma(\mathrm{arom},i-1)}\epsilon) \times \cos^2[\pi\,{}^3J_{NC\gamma(\mathrm{arom},i)}(\delta + \tau_{90°,C'} + \epsilon)], \quad [2]$$

respectively. The inevitably different dephasing times for the two coupling types perfectly match their unequal average magnitudes.

Quantitative ^3J determination requires reference signal intensities to be measured, usually in separate experiments where the desired couplings are refocused while an otherwise identical magnetization transfer pathway is employed. Here we follow a different strategy, which has recently been described

1090-7807/00 $35.00

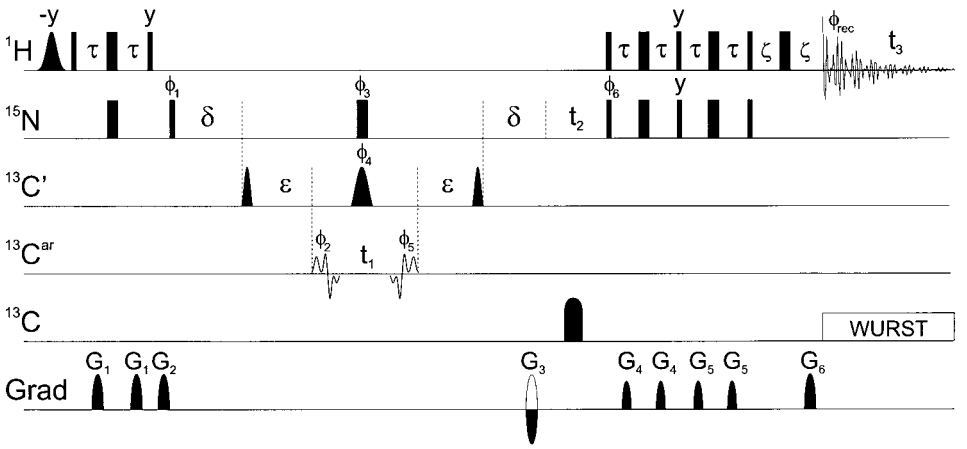

FIG. 1. Experimental scheme for the simultaneous measurement of $^3J_{N,C\gamma(atom)}$ and $^3J_{C',C\gamma(arom)}$ coupling constants. Narrow and wide RF pulses have flip angles of 90° and 180°, respectively, and are applied with phase *x* unless otherwise specified. All proton pulses are applied at the water resonance (4.75 ppm). The initial 90° Gaussian shaped pulse (duration: 2.5 ms) aligns the water magnetization along the positive *z* axis at the end of the sequence and avoids the saturation of fast exchanging amide protons by pulsed field gradients (*9–11*). The ^{15}N and ^{13}C carrier frequencies are centered in the amide (121 ppm) and aromatic (124 ppm) spectral region, respectively. Pulses on ^{13}C′ and ^{13}C are applied at 176.5, and 108 ppm, respectively, using phase modulation (*12*). Carbonyl-selective 90° and 180° pulses pulses are shaped according to the center lobe of a $\sin(x)/x$ function and have a duration of 200 μs. Band selective excitation of aromatic carbons is accomplished by G^4 Gaussian cascades (*13*) with a duration of 500 μs. The second G^4 pulse has a time-reversed envelope, and its phase is empirically adjusted to compensate for zero-order phase shifts induced by the 180° ^{13}C′ pulse in the t_1 evolution period (23° in the present implementation). Scalar nitrogen–carbon couplings during t_2 are refocused by a 1-ms WURST-20 (*14*) inversion pulse (50 kHz sweep) on ^{13}C while optional decoupling during acquisition in order to eliminate proton–carbon long-range couplings is achieved by a sequence of 3-ms WURST pulses, employing a five-step supercycle (*15*). Delays τ and ζ are adjusted to 2.3 and 0.7 ms, respectively. De- and rephasing of $^3J_{N,C\gamma}$ and $^3J_{C',C\gamma}$ interactions occurs during the periods $(\delta + \tau_{90°,C'} + \epsilon)$ and ϵ, respectively. To compensate for ^{15}N chemical shift evolution during the ^{13}C WURST-20 pulse, a duration of $\tau_{180°,C}/2$ is added to the first and is subtracted from the second δ delay, avoiding a first-order phase correction in the F_2 dimension. Quadrature detection in t_1 is accomplished by altering ϕ_2 in the States (*16*) manner. Phase cycles (verified for our Bruker Avance spectrometer) are $\phi_1 = x$; $\phi_2 = x$; $\phi_3 = 2(x), 2(y)$; $\phi_4 = x, y, -x, -y$; $\phi_5 = -x$; $\phi_6 = x$; $\phi_{receiver} = x, 2(-x), x$ for the real part and $\phi_1 = x$; $\phi_2 = y$; $\phi_3 = 2(x), 2(y)$; $\phi_4 = x, y, -x, -y$; $\phi_5 = 4(-x), 4(x)$; $\phi_6 = x$; $\phi_{receiver} = x, 2(-x), x, -x, 2(x), -x$ for the imaginary part of each t_1 increment. At other spectrometer types it may be necessary to invert the phases of the selective and of the second 90° hard pulse on protons to constructively add components originating from ^{1}H and ^{15}N steady-state magnetizations (*17*). Gradients are sine-bell shaped and have the following durations, peak amplitudes, and directions: G_1, 1 ms, 5 G/cm, *x*; G_2, 1 ms, 10 G/cm, *y*; G_3, 1 ms, −39.5 G/cm, *xyz*; G_4, 0.5 ms, −4 G/cm, *xy*; G_5, 0.5 ms, −5.5 G/cm, *xy*; G_6, 0.5 ms, 8 G/cm, *xyz*. N- and P-type signals are collected alternately by inverting the polarity of G_3 along with phase ϕ_6. Axial peaks in the ^{15}N dimension are shifted to the edge of the spectrum by incrementing ϕ_1 and the receiver phase by 180° for each value of t_2.

in detail (*18*). Briefly, two different phase cycles are employed for recording the real ($\phi_2 = x$) and imaginary ($\phi_2 = y$) parts of each t_1 increment, in such a manner that magnetization which is not transferred to aromatic carbons is rejected only in the latter. This fraction, which is proportional to

$$\sin^2(\pi^1 J_{NC'}\delta) \times \cos^2[\pi^3 J_{NC\gamma(arom)}(\delta + \tau_{90°,C'} + \epsilon)] \times \cos^2(\pi^3 J_{C'C\gamma(arom)}\epsilon), \quad [3]$$

gives rise to signals void of chemical-shift modulation. In the final 3D spectrum, therefore, signals appearing in the axial-peak plane at $\omega_1 = 0$ can be exploited as internal reference to calculate coupling constants according to

$$I_{cross,C\gamma(i)}/I_{axial} = \tan^2[\pi^3 J_{NC\gamma(arom)}(\delta + \tau_{90°,C'} + \epsilon)] \quad [4]$$

and

$$I_{cross,C\gamma(i-1)}/I_{axial} = \tan^2(\pi^3 J_{C'C\gamma(arom)}\epsilon). \quad [5]$$

Note that, in contrast to homonuclear quantitative *J* correlations where cross and reference peaks have opposite signs, the relative signs can be arbitrarily chosen here by the adjustment of pulse phases ϕ_2/ϕ_5.

In a similar approach, axial peaks, albeit recorded separately, had been used as reference in long-range ^{1}H–^{13}C correlation spectra (*19*). Furthermore it should be mentioned that in projected triple-resonance spectra, axial peaks proved to be useful as central peaks facilitating symmetrization (*20*).

Owing to the long period of ^{15}N transverse relaxation in the modified HN(CO)CG experiment described here, it lends itself to TROSY-type (*6, 7*) suppression of transverse relaxation, which has already been exploited to enable observation of scalar couplings across hydrogen bonds in larger biomolecules (*21–23*). In the pulse sequence of Fig. 1 the [^{15}N, ^{1}H]-TROSY coherence transfer has been implemented in the gradient selected, sensitivity enhanced (*24–30*) manner, employing the improved scheme of Ref. (*31*). In the present application no active suppression of the unwanted anti-TROSY component is

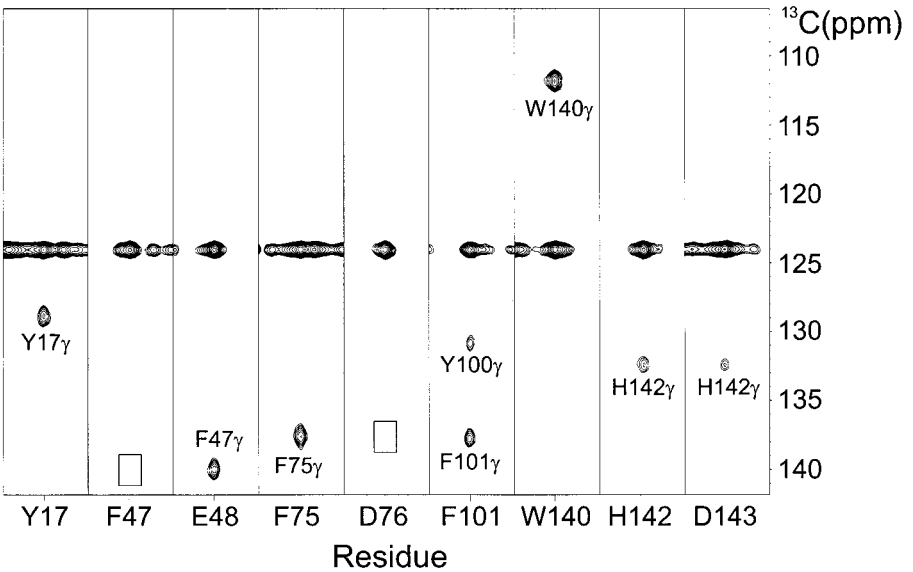

FIG. 2. (F1/F3) strips from HN(CO)CG-[^{1}H, ^{15}N]-TROSY spectra (^{1}H frequency: 800.13 MHz) of ^{13}C/^{15}N-labeled flavodoxin taken at the ^{15}N (F_2) chemical shifts and centered at the $^{1}H^{N}$ (F_3) frequencies of the residues indicated at the bottom. The width along F_3 of each strip is 0.25 ppm. Contour levels are drawn on an exponential scale using a factor of $2^{1/2}$. Intensity ratios between cross peaks involving the aromatic γ-carbons of the either the same or the preceding residue and axial peaks appearing at the center of the ^{13}C (F_1) dimension are employed to calculate $^{3}J_{N,C\gamma}$ and $^{3}J_{C',C\gamma}$ coupling constants, respectively. In the case of missing cross peaks, indicated by empty rectangular boxes, only upper limits of the coupling constants can be derived from the noise level and axial peak intensities.

required, as it decays below the detection threshold during delays δ and ϵ. To maximize sensitivity and resolution with regard to the TROSY approach, the experiment is preferably performed at the highest magnetic fields currently available (*6*). On the other hand, this is accompanied by an accelerated decay of transverse $^{13}C'$ magnetization during the ϵ periods because of the relatively large contribution of CSA to carbonyl relaxation. Under some conditions, e.g., if conformational exchange appreciably contributes to ^{15}N relaxation, it might therefore be beneficial to run the experiment in a non-TROSY fashion at lower field.

In order to avoid a signal decay in t_2, the evolution time might be superimposed on the δ delays in a constant-time manner, but this would require the introduction of additional ^{15}N and ^{13}C 180° pulses, imperfections of which compromise the accuracy of the ^{3}J quantification. Considering the slow transverse ^{15}N relaxation in TROSY, it was found preferable to record nitrogen chemical shifts in a conventional evolution time, thus minimizing the number of RF pulses.

The utility of the HN(CO)CG-[^{15}N, ^{1}H]-TROSY sequence is demonstrated with oxidized *Desulfovibrio vulgaris* flavodoxin, a bacterial redox protein consisting of 147 amino acid residues and a flavin-mononucleotide cofactor (MW: 16.3 kDa). To assess its precision, the experiment was repeated four times, using slightly different settings for delays δ and ϵ, varying between 30 and 32 ms and between 28 and 35 ms, respectively. Figure 2 shows strips from the resulting 3D spectra taken at the positions of the amides of aromatic amino acids or the respective succeeding residues. Coupling constants are obtained from intensity ratios of cross peaks at $^{13}C^{\gamma(arom)}$ resonance positions and axial peaks occurring at the center of the F_1 axis as described above. Note that the ^{13}C carrier frequency was chosen so as to avoid overlap between cross peaks and axial peaks. The resulting ^{3}J values for all 14 aromatic residues in flavodoxin are summarized in Table 1.

For the evaluation of coupling constants, peak heights rather than integrated signal intensities have been used here since the former can be measured more reliably, although identical line shapes within each cross/axial peak pair would be required theoretically. The fact that cross peaks but not axial peaks are broadened along the F_1 domain by one-bond ^{13}C, ^{13}C and long-range ^{1}H, ^{13}C couplings involving the $^{13}C^{\gamma}$ spins therefore results in an underestimation of $^{3}J_{N,C\gamma}$ and $^{3}J_{C',C\gamma}$. Unfortunately, the largest of these passive couplings, i.e., $^{1}J_{C\gamma,C\delta}$, cannot be eliminated whereas refocusing of $^{1}J_{C\gamma,C\beta}$ would be feasible. Restricting the $^{13}C^{\gamma}$ evolution time to less than 6 ms in combination with apodization, however, keeps the effect of all passive couplings relatively small (7–8%). Application of a selective refocusing pulse on β-carbons in the center of t_1, which would further delay acquisition in this domain and induce a Bloch–Siegert effect on carbonyls, was disregarded for these reasons. The evolution of ^{1}H, $^{13}C^{\gamma}$ interactions is avoided in a non-TROSY version of the pulse sequence, using proton composite pulse decoupling; however, they have only a negligible effect on cross peak heights with the chosen t_1 acquisition time. Another possible source of systematic error is

TABLE 1

Experimental $^{3}J_{NC\gamma}$ and $^{3}J_{C'C\gamma}$ Coupling Constants and X-Ray Crystallographic (*32*) Sidechain χ1 Angles for Aromatic Residues in *Desulfovibrio vulgaris* Flavodoxin

	$\lvert^{3}J_{NC\gamma}\rvert$ (Hz)[a]	$^{3}J_{C'C\gamma}$ (Hz)[a]	χ1 (°)
Y8	<0.5[b]	<1.0[b]	65.5
Y17	1.88 ± 0.08	<0.9[b]	164.6
Y31	<0.5[b]	2.46 ± 0.12	−80.9
F47	<0.5[b]	4.04 ± 0.07	−49.5
F50	<0.4[b]	3.34 ± 0.10	−77.3
W60	<0.8[b]	<1.8[b]	−64.8
F71	1.43 ± 0.08	<0.8[b]	−151.8
F75	2.01 ± 0.07	<0.8[b]	−176.3
F91	<0.5[b]	<1.2[b]	54.2
Y98	<0.4[b]	2.94 ± 0.20	−71.8
Y100	—[c]	2.94 ± 0.16	−56.5
F101	2.13 ± 0.09	<1.3[b]	172.2
W140	2.33 ± 0.01	<0.8[b]	−176.5
H142	1.34 ± 0.02	2.07 ± 0.08	−109.6

[a] Averages and standard deviations resulting from four separate measurements. Values are not corrected for $^{13}C^{\gamma}$ spin flips or different line widths of cross and axial peaks.

[b] Upper limit derived from axial peak intensities in the absence of cross peaks.

[c] Intensity of reference peak could not be determined due to spectral overlap.

differential relaxation of magnetization terms associated with cross and axial peaks arising from C$^{\gamma}$ spins flips during the δ and ϵ periods. Assuming a T_1 time of 1 s for the unprotonated γ-carbons of aromatic amino acids, it can be calculated (*33*) that the apparent coupling constants as determined directly from intensity ratios underestimate their true values by less than 4% for $^{3}J_{N,C\gamma}$ and less than 3% for $^{3}J_{C',C\gamma}$ in their entire respective accessible ranges.

While Karplus curves for the two couplings remain to be determined, $^{3}J_{N,C\gamma}$ and $^{3}J_{C',C\gamma}$ values around 2.4 and 4.0 Hz for *trans* and ≤0.5 and ≤1.1 Hz for gauche conformations were reported (*3*). For the majority of the aromatic residues in flavodoxin either $^{3}J_{N,C\gamma}$ or $^{3}J_{C',C\gamma}$, or both, was too small (i.e., smaller than approximately 0.5 and 1.0 Hz, respectively) to give rise to an observable cross peak, in accordance with χ1 angles close to one of the three staggered rotamers. An exception is His142, where cross peaks due to both $^{3}J_{N,C\gamma}$ and $^{3}J_{C',C\gamma}$ were detected, which is indicative for a skewed conformation or χ1 rotamer averaging. In almost all instances, measured coupling constants agree well with torsion angles in the X-ray structure of flavodoxin (*32*). In contrast, a large $^{3}J_{C',C\gamma}$ value is expected for Trp60 on the basis of its side chain conformation in the crystal, but it could not be measured here. However, unusually low intensities were observed for the axial peaks of Trp60 and the sequentially following Gly61, both of which are located in the flavin binding site. For these two residues, significant backbone conformational exchange had been detected by ^{15}N relaxation in the oxidized state of the protein (*34*).

It should be mentioned that spectral overlap may limit application of the novel HN(CO)CG-type experiment, since all reference signals are located in the center (^{1}H, ^{15}N)-plane of a 3D spectrum. However, as only relatively few data points need to be recorded in the ^{13}C dimension, a ^{15}N resolution not substantially lower than in 2D ^{15}N- or $^{13}C'$-{$^{13}C^{\gamma}$} spin–echo difference ^{1}H–^{15}N HSQC experiments (*3*) can be achieved. In the case of flavodoxin the intensity of only one relevant axial peak could not be measured due to nearly complete degeneracy of ^{1}H and ^{15}N chemical shifts with those of another amide. Note that in a 2D spin–echo difference type experiment a simultaneous determination of $^{3}J_{N,C\gamma}$ and $^{3}J_{C',C\gamma}$ for two sequentially adjacent aromatic residues is impossible because scalar interactions involving the two respective γ-carbons would be indistinguishable. As demonstrated in Fig. 2 this ambiguity is easily resolved for the residue pair Tyr100/Phe101 by recording $^{13}C^{\gamma}$ chemical shifts in the third dimension.

CONCLUSIONS

A sensitive pulse sequence has been introduced which allows the measurement of $^{3}J_{N,C\gamma}$ and $^{3}J_{C',C\gamma}$ coupling constants in aromatic amino acids from a single spectrum. This was achieved by combining the N–C′, N–C$^{\gamma}$, and C′–C$^{\gamma}$ de- and rephasing periods of the HN(CO)CG sequence, as well as by adding a TROSY detection scheme. Separate recording of reference spectra was no longer needed owing to the use of a novel phase cycling scheme. The method would be especially suitable for application to perdeuterated proteins, the more so because χ1 angle information from other couplings or intraresidual NOE is unavailable here.

EXPERIMENTAL

The HN(CO)CG-[^{15}N, ^{1}H]-TROSY pulse sequence was applied to a 1.4 mM sample of $^{13}C/^{15}N$ labeled *Desulfovibrio vulgaris* flavodoxin dissolved in 0.5 ml 10 mM potassium phosphate buffer (pH 7) containing 5% D_2O. The experiment was carried out four times with different values of delays δ and ϵ. Furthermore, spectral widths in the ^{15}N dimension were varied in order to take accidental overlap of aliased and unaliased axial peaks into account.

In detail, parameters in each of the data sets were: (1) δ = 30 ms, ϵ = 28 ms, SW (F_2) = 14.7 ppm, ^{15}N acquisition time = 53.6 ms; (2) δ = 32 ms, ϵ = 32 ms, SW (F_2) = 14.7 ppm, ^{15}N acquisition time = 53.6 ms; (3) δ = 30 ms, ϵ = 30 ms, SW (F_2) = 12.0 ppm, ^{15}N acquisition time = 65.8 ms; (4) δ = 32 ms, ϵ = 35 ms, SW (F_2) = 12.5 ppm, ^{15}N acquisition time = 63.1 ms. Spectral widths in F_1 (^{13}C) and F_3 (^{1}H) comprised 38.2 and 10.4 ppm, respectively. Time domain data consisted of 44 × 64 × 768 (t_1, t_2, t_3) complex points,

corresponding to acquisition times of 5.7 ms in the ^{13}C dimension and 92.2 ms in the ^{1}H dimension. All spectra were recorded on a Bruker DRX-800 spectrometer equipped with a 5-mm three-axis gradient $^{1}H\{^{13}C, ^{15}N\}$ triple-resonance probe with the temperature set at 27°C. Accumulation of eight scans per FID resulted in a recording time of 32 h for each data set.

Processing and spectra analysis was carried out using the NMRPipe/NMRDraw (*35*) software. Linear prediction was employed to extend time domain data in the ^{13}C and ^{15}N dimensions by 16 and 40 points, respectively. Before Fourier transformation, data in all three dimensions were multiplied with a squared-cosine weighting function and were zero-filled to obtain a final data set size of 256 × 256 × 2048 real points.

ACKNOWLEDGMENTS

We thank Professor S.G. Mayhew (Department of Biochemistry, University College Dublin) and Dr. M. Knauf for their support with the expression and labeling of the *D. vulgaris* flavodoxin. This work was supported by a grant from the Deutsche Forschungsgemeinschaft (Ru 145/11-2).

REFERENCES

1. D. Yang, Y.-K. Mok, D. R. Muhandiram, J. D. Forman-Kay, and L. E. Kay, $^{1}H–^{13}C$ dipole–dipole cross-correlated spin relaxation as a probe of dynamics in unfolded proteins: Application to the DrkN SH3 domain, *J. Am. Chem. Soc.* **121,** 3555–3556 (1999).
2. M. Hennig, W. Bermel, A. Spencer, C. M. Dobson, L. J. Smith, and H. Schwalbe, Side-chain conformations in an unfolded protein: $\chi 1$ distributions in denatured hen lysozyme determined by heteronuclear ^{13}C, ^{15}N NMR spectroscopy, *J. Mol. Biol.* **288,** 705–723 (1999).
3. J.-S. Hu, S. Grzesiek, and A. Bax, Two-dimensional NMR methods for determining $\chi 1$ angles of aromatic residues in proteins from three-bond $J_{C'C\gamma}$ and $J_{NC\gamma}$ couplings, *J. Am. Chem. Soc.* **119,** 1803–1804 (1997).
4. R. Konrat, D. R. Muhandiram, N. A. Farrow, and L. E. Kay, Pulse schemes for the measurement of $^{3}J_{C'C\gamma}$ and $^{3}J_{NC\gamma}$ scalar couplings in ^{15}N, ^{13}C uniformly labeled proteins, *J. Biomol. NMR* **9,** 409–422 (1997).
5. A. Bax, G. W. Vuister, S. Grzesiek, F. Delaglio, A. C. Wang, R. Tschudin, and G. Zhu, Measurement of homo- and heteronuclear *J* couplings from quantitative *J* correlation, *Methods Enzymol.* **239,** 79–105 (1994).
6. K. Pervushin, R. Riek, G. Wider, and K. Wüthrich, Attenuated T_2 relaxation by mutual cancellation of dipole–dipole coupling and chemical shift anisotropy indicates an avenue to NMR structures of very large biological macromolecules in solution, *Proc. Natl. Acad. Sci. USA* **94,** 12366–12371 (1997).
7. M. Salzmann, K. Pervushin, G. Wider, H. Senn, and K. Wüthrich, TROSY in triple-resonance experiments: New perspectives for sequential NMR assignment of large proteins, *Proc. Natl. Acad. Sci. USA* **95,** 13585–13590 (1998).
8. J.-S. Hu and A. Bax, Determination of ϕ and $\chi 1$ angles in proteins from $^{13}C–^{13}C$ three-bond *J* couplings measured by three-dimensional heteronuclear NMR. How planar is the peptide bond?, *J. Am. Chem. Soc.* **119,** 6360–6368 (1997).
9. S. Grzesiek and A. Bax, The importance of not saturating H_2O in protein NMR. Application to sensitivity enhancement and NOE measurements, *J. Am. Chem. Soc.* **115,** 12593–12594 (1993).
10. J. Stonehouse, G. L. Shaw, J. Keeler, and E. D. Laue, Minimizing sensitivity losses in gradient-selected $^{15}N–^{1}H$ HSQC spectra of proteins, *J. Magn. Reson. Ser. A* **107,** 178–184 (1994).
11. H. Matsuo, Ē. Kupče, H. Li, and G. Wagner, Use of selective C^{α} pulses for improvement of HN(CA)CO-D and HN(COCA)NH-D experiments, *J. Magn. Reson. Ser. B* **111,** 194–198 (1996).
12. S. L. Patt, Single- and multiple-frequency-shifted laminar pulses, *J. Magn. Reson.* **96,** 94–102 (1992).
13. L. Emsley and G. Bodenhausen, Gaussian pulse cascades: New analytical functions for rectangular selective inversion and in-phase excitation in NMR, *Chem. Phys. Lett.* **165,** 469–476 (1990).
14. Ē. Kupče and R. Freeman, Adiabatic pulses for wideband inversion and broadband decoupling, *J. Magn. Reson. Ser. A* **115,** 273–276 (1995).
15. R. Tycko, A. Pines, and R. Guckenheimer, Fixed point theory of iterative excitation schemes in NMR, *J. Chem. Phys.* **83,** 2775–2802 (1985).
16. D. J. States, R. A. Haberkorn, and D. J. Ruben, A two-dimensional nuclear Overhauser experiment with pure absorption phase in four quadrants, *J. Magn. Reson.* **48,** 286–292 (1982).
17. K. Pervushin, R. Riek, G. Wider, and K. Wüthrich, Transverse relaxation-optimized spectroscopy (TROSY) for NMR studies of aromatic spin systems in ^{13}C-labeled proteins, *J. Am. Chem. Soc.* **120,** 6394–6400 (1998).
18. F. Löhr, C. Pérez, J. M. Schmidt, and H. Rüterjans, Recording heteronuclear quantitative *J*-correlation spectra with internal reference peaks, *Bull. Magn. Reson.* **20,** 9–14 (1999).
19. G. Zhu and A. Bax, Measurement of long-range $^{1}H–^{13}C$ coupling constants from quantitative 2D heteronuclear multiple-quantum correlation spectra, *J. Magn. Reson. Ser. A* **104,** 353–357 (1993).
20. T. Szyperski, D. Braun, B. Banecki, and K. Wüthrich, Useful information from axial peak magnetization in projected NMR experiments, *J. Am. Chem. Soc.* **118,** 8146–8147 (1996).
21. A. J. Dingley and S. Grzesiek, Direct observation of hydrogen bonds in nucleic acid base pairs by internucleotide $^{2}J_{NN}$ couplings, *J. Am. Chem. Soc.* **120,** 8293–8297 (1998).
22. K. Pervushin, A. Ono, C. Fernández, T. Szyperski, M. Kainosho, and K. Wüthrich, NMR scalar couplings across Watson–Crick base pair hydrogen bonds in DNA observed by transverse relaxation-optimized spectroscopy, *Proc. Natl. Acad. Sci. USA* **95,** 14147–14151 (1998).
23. Y.-X. Wang, J. Jacob, F. Cordier, P. Wingfield, S. J. Stahl, S. Lee-Huang, D. Torchia, S. Grzesiek, and A. Bax, Measurement of $^{3h}J_{NC'}$ connectivities across hydrogen bonds in a 30 kDa protein, *J. Biomol. NMR* **14,** 181–184 (1999).
24. M. Czisch and R. Boelens, Sensitivity enhancement in the TROSY experiment, *J. Magn. Reson.* **134,** 158–160 (1998).
25. P. Andersson, A. Annila, and G. Otting, An α/β-HSQC-α/β experiment for spin-state selective editing of IS cross-peaks, *J. Magn. Reson.* **133,** 364–367 (1998).
26. K. V. Pervushin, G. Wider, and K. Wüthrich, Single transition to single transition polarization transfer (ST2-PT) in $[^{15}N, ^{1}H]$-TROSY, *J. Biomol. NMR* **12,** 345–348 (1998).
27. G. Zhu, X. Kong, X. Yan, and K. Sze, Sensitivity enhancement in transverse relaxation optimized NMR spectroscopy, *Angew. Chem. Int. Ed.* **37,** 2859–2861 (1998).
28. M. Rance, J. P. Loria, and A. G. Palmer III, Sensitivity improvement

of transverse relaxation-optimized spectroscopy, *J. Magn. Reson.* **136,** 92–101 (1999).

29. J. Weigelt, Single scan, sensitivity- and gradient-enhanced TROSY for multidimensional NMR experiments, *J. Am. Chem. Soc.* **120,** 10778–10779 (1998).

30. B. Brutscher, J. Boisbouvier, A. Pardi, D. Marion, and J.-P. Simorre, Improved sensitivity and resolution in ^{1}H–^{13}C NMR experiments of RNA, *J. Am. Chem. Soc.* **120,** 11845–11851 (1998).

31. D. Yang and L. E. Kay, Improved ^{1}HN-detected triple resonance TROSY-based experiments, *J. Biomol. NMR* **13,** 3–10 (1999).

32. W. Watt, A. Tulinsky, R. P. Swenson, and K. D. Watenpaugh, Comparison of the crystal structures of a flavodoxin in its three oxidation states at cryogenic temperatures, *J. Mol. Biol.* **218,** 195–208 (1991).

33. G. W. Vuister and A. Bax, Quantitative *J* correlation: A new approach for measuring homonuclear three-bond $J(H^{N}H^{\alpha})$ coupling constants in ^{15}N-enriched proteins, *J. Am. Chem. Soc.* **115,** 7772–7777 (1993).

34. A. Hrovat, M. Blümel, F. Löhr, S. G. Mayhew, and H. Rüterjans, Backbone dynamics of oxidized and reduced *D. vulgaris* flavodoxin in solution, *J. Biomol. NMR* **10,** 53–62 (1997).

35. F. Delaglio, S. Grzesiek, G. W. Vuister, G. Zhu, J. Pfeifer, and A. Bax, NMRPipe: A multidimensional spectral processing system based on UNIX pipes, *J. Biomol. NMR* **6,** 277–293 (1995).